AALBORG UNIVERSITY

DENMARK

Prediction and Validation of Wear-Out Reliability Metrics for Power Semiconductor Devices With Mission Profiles in Motor Drive Application

Ma, Ke; Choi, Ui-Min; Blaabjerg, Frede

Prediction and Validation of Wear-out Reliability Metrics for Power Semiconductor Devices with Mission Profiles in Motor Drive Application

Ke Ma[1], Ui-Min Choi[2,3], Frede Blaabjerg[3]

1. Department of Electrical Engineering, Shanghai Jiao Tong University, Shanghai 200240, China
2. Department of Electronic and IT Media Engineering, Seoul National University of Science and Technology, Korea
3. Department of Energy Technology, Aalborg University, Aalborg DK-9220, Denmark

kema@sjtu.edu.cn, uch@et.aau.dk, fbl@et.aau.dk

Abstract – **Due to the continuous demands for highly reliable and cost-effective power conversion, quantified reliability performances of the power electronics converter are becoming emerging needs. The existing reliability predictions for the power electronics converter mainly focus on the metrics of lifetime, accumulated damage, constant failure rate or Mean-Time-To-Failure (MTTF). Nevertheless, the time-varying and probability-distributed characteristics of the reliability, are rarely involved. Moreover, in the public literatures, there are few evidences showing that the accuracy of the predicted reliability was experimentally validated. In this paper, a more advanced metric "Cumulative Distribution Function (CDF)" is introduced to predict the reliability performance of power electronics system based on mission profiles in motor drive application. Furthermore, the accuracy of the predicted reliability metrics is verified through a series of wear-out tests in a converter testing system. It is concluded that the CDF is a very suitable metric to predict the reliability performance of converter, and it has shown good accuracy with much more reliability information compared to the existing approaches. In this method, the correct stress translation and dedicated strength tests based on mission profiles are two key factors to ensure the efficiency and accuracy of reliability prediction.**

I. INTRODUCTION

Power electronics have been widely installed in emerging applications of energy conversion such as renewables, motor drives, aircrafts, power transmission, etc., in these applications the reliability requirements for the power conversion system are becoming more and more strict [1]-[7]. In order to satisfy the stringent reliability requirements, meanwhile to limit the development cost and reduce the testing time, there are strong demands for more accurate prediction of the reliability performances in power electronics components and systems.

Different from the widely used metrics for the power electronics converter such as efficiency, power density, Total Harmonics Distortion (THD), etc., reliability is a performance which is difficult to quantify and characterize. In a conventional approach to assess the reliability performance of power electronics system, the reliability information is decided at component level based on the statistics of large number of failed products. Afterwards the constants of failure-rate or Mean Time To Failure (MTTF) for various components are established in some handbooks [8], [9], which are used to calculate the failure-rate or MTTF of the whole converter according to the connecting logics of multiple components or sub systems [10]-[16]. Nowadays, this "MTTF prediction" or

"constant failure-rate prediction" approach has been discouraged for the reliability assessment of power electronics, since it is mission profiles independent and the accuracy is hard to be ensured, as specified in [3], [17].

Motivated by the growing reliability demands in the mission-critical applications of power electronics, new approaches considering mission profiles for the reliability prediction has been initialized based on Physic-of-Failure (PoF) of component since 1990s' [3], [18], [19]. A series of important failure mechanisms for power semiconductor devices were investigated and modelled, and the thermal cycling was identified as one of the most important causes of failures [20]-[23]. The lifetime of power semiconductor devices was characterized by means of accelerated tests [24]-[28], and many lifetime models have been developed based on various complexities of the thermal cycles [29]-[32], or based on different packing technologies of devices [33], [34]. A typical example from the pioneering work in 1997 is shown in [28], which is based on a series of accelerated tests of IGBT modules. In this work the metrics of B10 percentile lifetime (i.e. the number of cycles or time at which the device has 10 % probability of failure) are provided at multiple thermal stress levels, such as swing amplitudes ΔT_j and mean values T_m. This lifetime-stress relationship is also referred as lifetime models of components.

Recently, a series of works have been found to utilize these lifetime models in order to better predict the reliability of converters based on different mission profiles and applications [35]-[38]. In these "lifetime prediction" approaches for the reliability assessment of power electronics, the mission profiles are correlated with the reliability performances, and the accuracy of the predicted results strongly depends on the used lifetime models of components. Some critical limitations in this "lifetime prediction" approach can be identified as: 1. For most of the existing lifetime models, the device is loaded passively or with DC current pulses to emulate limited ranges of thermal-stress intensities. The testing conditions are normally different from the real-field applications, where the characteristics of the thermal cycles are much more complex. 2. The technology and manufacturing of power semiconductor devices have been advanced continuously, some of the lifetime models, which were built decades ago, need to be updated. 3. Only constants of lifetime are provided in these lifetime models, the time-varying and probability-distributed characteristics of the
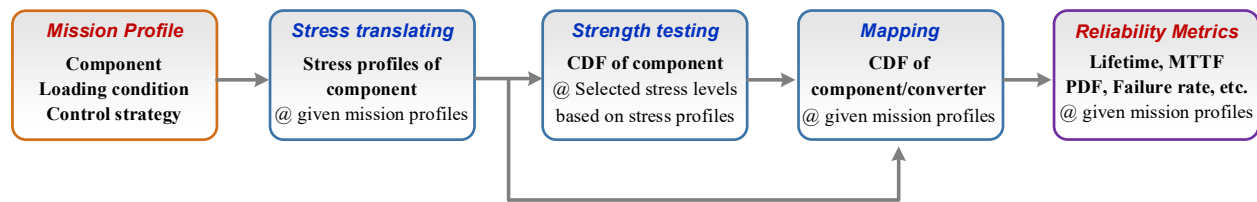
Fig. 1. Flow to acquire the CDF and reliability metrics of power electronics converter based on given mission profiles.

reliability are lost. Consequently, there is still no evidence in public literatures showing that the accuracy of these predicted lifetimes of converter was experimentally verified.

This paper serves to introduce more advanced metrics and more efficient methods to predict the reliability performances of power electronics under certain mission profiles. Furthermore, the accuracy of the predicted reliability metrics, as well as the key factors to ensure the accuracy and efficiency of reliability prediction, are experimentally explored. The analyzing scenario is based on the wear-out failure mechanism of bond-wire lift-off in power semiconductors, which are stressed with thermal cycles experienced in a motor drive application.

II. KEY RELIABILITY METRIC CDF AND PREDICTION FLOW

A time-varying variable $R(t)$ with the unit of % is normally used to quantify the reliability performance of component or system in the field of reliability engineering. $R(t)$ represents the percentage of a group of samples (or the probability of one sample) that can properly function at operating time t. Similarly, the unreliability or probability of failure $F(t)$ can be defined as percentage of a group of samples that fail at operating time t. The plot of $F(t)$ against the operating time t is referred as Cumulative Distribution Function (CDF) curve, which in most of the cases increases with time and can be represented by an analytical function developed in 1951 by Walloddi Weibull [40]. This fitting function is also known as Weibull distribution function.

Compared to the metrics of constants including MTTF or lifetime, which are widely used in the existing approaches for reliability prediction of power electronics, the metric of variable CDF provides more information about the reliability performance, especially the time-varying and probability-distributed characteristics. Therefore, the CDF of a power electronics component/system is set as the prediction target in this paper. It is noted that the metric of CDF has already been successfully applied in the field of reliability engineering. However, CDF in that field is normally generated based on statistics of failed components/products, and it is used to describe the behaviors of failures which have already happened. In this paper, the CDF is used for prediction of failures that have not yet happened, and the CDF is generated based on a given mission profile of converter, as well as a series of models and designed tests.

In this paper, the flow to predict the CDF of converter is summarized in Fig. 1:

1. The critical stress profiles experienced by critical components are first translated from the given mission profiles of converter, such as the characteristics of

component, loading condition, and the control strategies, etc..

2. The CDF of the components is tested and extracted under carefully selected stress levels to reveal the strength information of components. Based on the pre-known stress profiles extracted from the previous step, the stress levels and number of samples for tests can be limited in a relatively small but effective range – this is significantly different from the existing approaches of strength tests where the testing conditions are relatively independent of the actual loading conditions and mission profiles.

3. A series of algorithms and calculation methods from the reliability engineering are applied to map the overall CDF of the component/converter based on the given mission profiles and stress/strength information extracted in the previous steps.

4. Other reliability metrics, such as lifetime, MTTF, failure rate, Probability Density Function (PDF), etc., can be deducted from the acquired CDF of components/converter under the given mission profiles.

III. PRE-ASSUMPTIONS AND HARDWARE TOOLS FOR ANALYSIS

There are several types of failures which are related to different aspects of reliability performance in a power electronics system, as explained in [41]. In this paper, the wear-out failures of components in the end of life of converter are to be analyzed, this is because the behaviors of failure in this period are very useful information to guide the design and warranty, and they can be more clearly identified and tested. It has been revealed that the thermal cycle is a critical stressor leading to the wear-out failures of power semiconductor devices, and the failure modes include bond-wire lift-off and soldering fatigues [22]. This paper will put focus on the introduction of more advanced reliability metrics to predict and validate the wear-out behaviors of power semiconductors under given mission profiles. In respect to the investigations of critical components and failure mechanisms, which have been well discussed in the past work [48], [51]-[53], are out of the scope of this paper.

A dedicated hardware tool based on the motor drive application is built to demonstrate and validate the reliability prediction method, as illustrated in Fig. 2. The setup is a three-phase circuit shared with common DC source, and each phase is composed of two-level H-bridge topology with individual inductor as the load. In each phase, one leg of the H-bridge is

used to generate the desired AC voltage of the system, and this leg is set as the Device Under Test (DUT), which is opened and black-painted to facilitate the chip temperature observation by infrared camera. The other leg of H-bridge is used to control the desired AC current flowing in the load inductor, and by this solution the DUT is operated at Sinusoidal-Pulse-Width Modulation (SPWM) mode to emulate the loading conditions close to the real-field operations, such as the voltage, current, power factor, switching frequency, modulation method and fundamental frequency. A thermal regulator is installed to control the temperature of the heatsink through coolant – by this approach the environmental temperatures of the converter system can be emulated, and the thermal impedance model can be simplified. The detail parameters of the setup are shown in Table I, which is based on a typical three-phase motor drive system. As an example to demonstrate the capability of the setup, the converter outputs under two operating conditions with different fundamental frequencies and power factors are shown in Fig. 3, it can be seen that the fundamental frequencies and power factors can be flexibly adjusted, and the power device is loaded actively under the similar condition in real field operation.
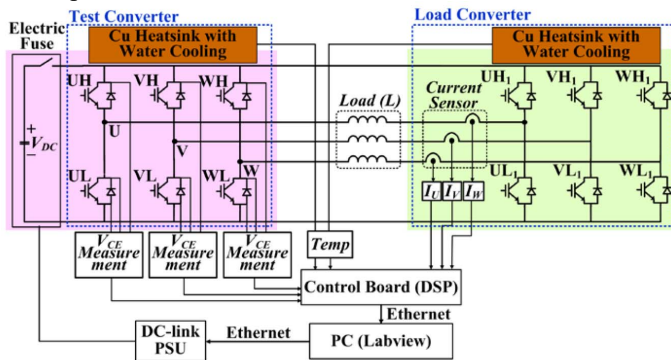

Fig. 2. Circuit diagram of the testing setup to demonstrate and validate the reliability metrics of IGBT module.

Table I. Parameters of the testing setup.

Parameters	Value
Max. convert power of DUT	7 kW
Peak AC voltage range	110-150 V
DC link voltage	400 V
Max. peak AC current	30 A
Fundamental frequency range	0.1-50 Hz
Max. switching frequency	15 kHz
3-phase IGBT Module DUT	600 V / 30 A
3-phase IGBT Module Loading	1200 V / 75A
Interface inductance	0.5 mH
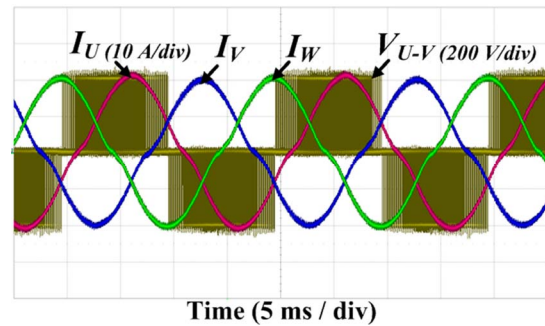
(a) fo = 50 Hz, PF = 1 (inverting mode).
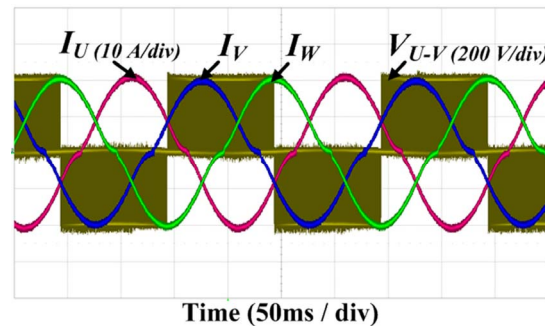
(b) fo = 5 Hz, PF = − 1 (rectifying mode).

Fig. 3. Outputs of the testing setup under various operating conditions when I_{peak} = 20 A.

IV. STRESS TRANSLATION OF THE COMPONENTS FROM MISSION PROFILES

One important step of the reliability prediction is to translate the mission profile of converter to the corresponding stress in the interested components, in the case of this paper, the thermal cycles in power semiconductor devices. This step can be done either by direct thermal measurement or monitoring during the operation of converter, or by multi-disciplinary modelling of the converter from system level to device level [4]. Due to the limitations for the accessibility of device as well as the flexibility of design improvement, the modelling approach is preferred compared to the monitoring method.

The thermal stress of the power semiconductor device is not only determined by the materials and thermal impedances, but is also determined by the behaviors of mechanical, control and electrical systems. Meanwhile other factors like the DC link voltage, cooling condition, and ambient temperature, etc. need to be taken into account. The comprehensive translation of mission profile to the thermal behaviors of power devices is a dedicated work requiring large efforts, this is out of the scope of this paper. Consequently, a simplified mission profile and operating condition in motor drive application is used, in order to keep the focus of this paper.

In the motor drive system, the fundamental frequency of the converter output normally varies intensively in a broad range as the speed and torque changes. This will lead to the disturbances in the cycling period of the thermal cycles. The duration time of the thermal cycle t_{period} is chosen as the targeting stress - this is different from the conventional

methods, in which the thermal stress of swing amplitude ΔT_j and mean level T_m are normally focused [32].

The modelling of electrical and control parts in the motor drive application have been extensively analyzed [43], [44]. Based on the electrical behaviors excited from the specifications shown in Fig. 2 and Table I, the power losses on individual chip of the power semiconductor devices can be calculated by using the switching and conduction characteristics shown in Fig. 4, these figures are experimentally extracted from the IGBT modules or DUT used in the testing setup.

(a)   Conduction characteristics of Transistor

(b) Conduction characteristics of freewheeling diode
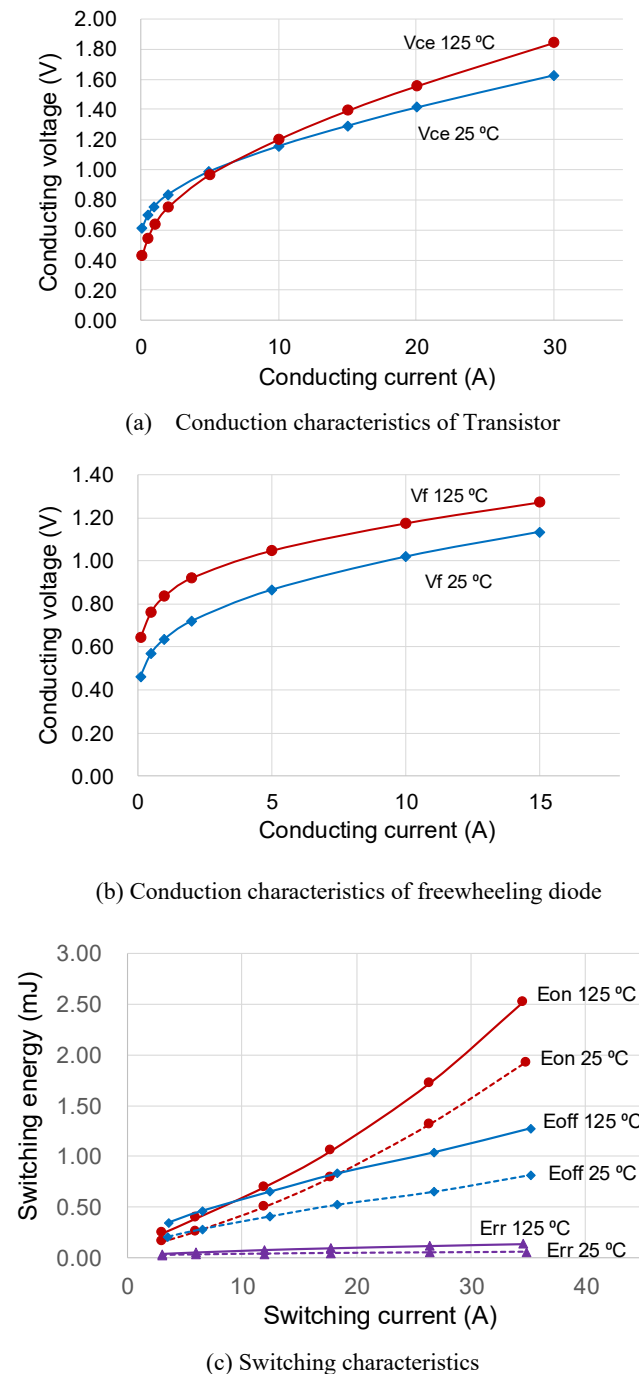

(c) Switching characteristics

Fig. 4. Conduction and switching characteristics of the IGBT module for study.

In order to extract the thermal impedance of the DUT, the construction and material of the used IGBT module is modeled under ANSYS to implement Finite Element Method (FEM) simulation, as shown in Fig. 5 (a) and Fig. 5 (b). The extracted parameters of the Foster type RC thermal networks between junction and case for the chip T_{VL} is illustrated, they are generated under a step power loss on chip T_{VL} from 0 to 10 W with ambient temperature fixed at 25 ℃, and the average temperature of the chip surface is set as junction temperature [47]. It is noted that the IGBT module used in this paper has no baseplate, and the heatsink temperature is controlled through a heater in coolant, thereby the Foster thermal impedance model for individual chip can be correctly used by connecting with the heatsink temperature. And the thermal coupling among chips can be ignored since the thermal coupling only dominates in the heatsink. If considering other types of IGBT module with baseplate, or considering the thermal disturbances from more complex mission profiles, more advanced thermal impedance models have to be used in the analysis [45], [46].
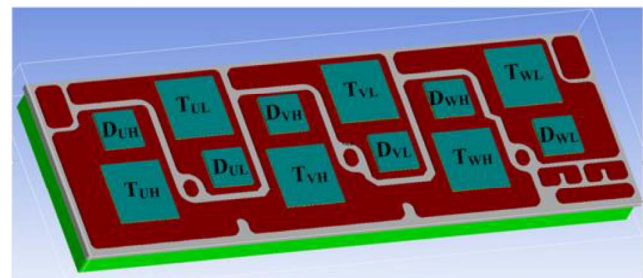
(a)   Construction of the FEM model
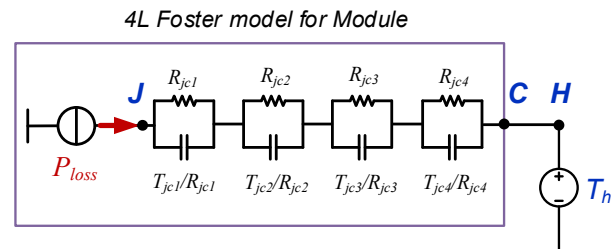
Parameters	Value
R_{jc1} (k/W)	0.6737
R_{jc2} (k/W)	0.6952
R_{jc3} (k/W)	0.3160
R_{jc4} (k/W)	0.0678
T_{jc1} (s)	0.123
T_{jc2} (s)	0.3905
T_{jc3} (s)	0.0188
T_{jc4} (s)	0.0009

(b) Extracted Foster type thermal impedance model of T_{VL}

Fig. 5. Thermal impedance model of the IGBT module for case study.

An infrared camera with sampling frequency of 300 Hz is installed to measure the average temperature of chip surface in DUT when the converter is loaded. The measured junction temperature on the transistor chip T_{VL} of DUT are shown in Fig.

6, where the fundamental frequency of the setup is set to 1 Hz with the operating condition of case 4 shown in Table II. The predicted thermal cycling by using the presented thermal stress models are also illustrated for comparison. It can be seen that the predicted thermal behavior generally follows the experimental measurements, although there is a small error around 6 % of the swing amplitude at the troughs – this may due to the factor that the heat sink temperature under test is actively controlled, and this condition is different from the one when characterizing the thermal model in the FEM simulation.
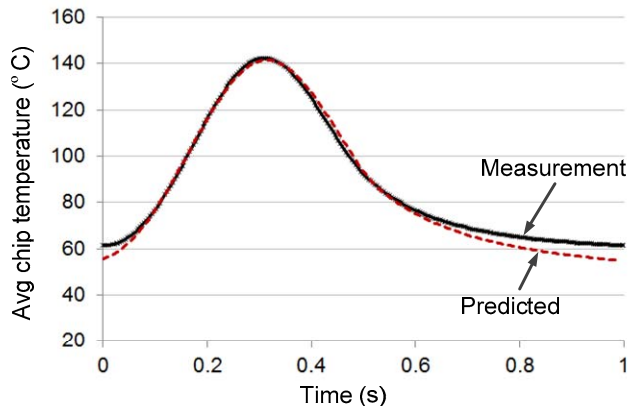

Fig. 6. Measured and predicted junction temperature on the transistor chip T_{VL} of tested IGBT module (measured as the average temperature on the chip surface by infrared camera, cycling frequency 1 Hz, heatsink temperature is controlled at 48 °C).
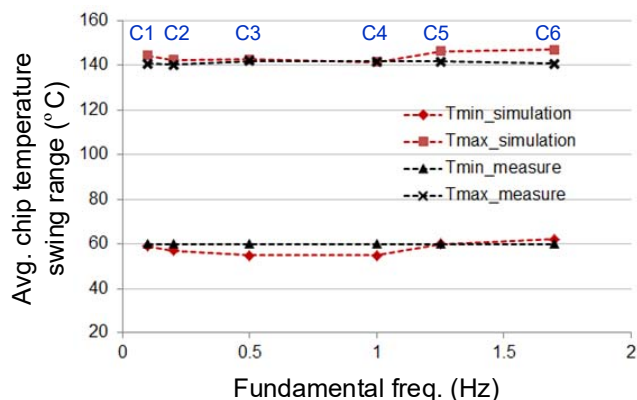

Fig. 7. Measured and predicted junction temperature ranges on the transistor chip T_{VL} with different cycling frequencies from Table II.

The swing ranges of the measured and predicted junction temperatures on T_{VL} under different fundamental frequencies are shown in Fig. 7, where the operating conditions of the setup are listed in Table II. These parameters cover majority range of the fundamental frequencies in the motor drive application based on the testing setup, and they can ensure the measured junction temperatures swing between 60 °C and 140 °C under all of the testing conditions. It can be seen that the error of the predictions under all of the conditions are within ± 5 °C compared to the experimental measurements. These errors could bring some uncertainties to the final predicted reliability metrics, and a series of sensitive analysis is needed to quantify the impacts to the predicted reliability performances. However, due to the length and scope of this paper, they are not implemented in this paper.

Table II. Operating conditions of testing setup under different thermal cycling frequencies

Condition	f_{out}	f_S	I_{max}	V_{refmax}	T_H
C1	0. 1 Hz	10 kHz	21 A	113 V	59 °C
C2	0.2 Hz	10 kHz	22 A	115 V	57 °C
C3	0.5 Hz	10 kHz	25 A	145 V	53 °C
C4	1 Hz	10 kHz	30 A	140 V	48 °C
C5	1.25 Hz	12 kHz	30 A	140 V	50 °C
C6	1.7 Hz	15 kHz	30 A	144 V	47 °C

f_{out}: fundamental frequency, f_s: switching frequency, I_{max}: load current peak, V_{refmax}: reference output AC voltage peak, T_H: controlled heat sink temperature.

V. CDF OF COMPONENTS UNDER DIFFERENT STRESS LEVELS

Another critical step for the reliability prediction of power electronics is to extracted strength information of components under different stress levels, this is normally done by accelerated tests of large number of components. There are two major limits in the existing methods: 1. For simplicity of tests, the testing conditions of devices are significantly different from the way that they are actually loaded in a converter; 2. The loading behaviors of device are not always specified, thereby many testing conditions of stress levels will be not experienced in practical use. Since the thermal behaviors focused in this paper have been investigated in the previous step, the testing conditions can be limited in a relatively small but effective range, according to the information indicated by the thermal profiles. Moreover, the accelerated tests are performed on the testing setup shown in Fig. 2, which can stress the devices closer to real-field.

A. Design of number of samples and the stress levels for strength test

Due to the trade-off between time/cost and uncertainty, the number of samples for the tested IGBT modules need to be carefully selected. Median Rank (*MR*) is one of the most used methods to quantify the uncertainty of small number of samples when generating a CDF curve [39]. *MR* is defined as a cumulative percentage of the population represented by a particular sample with 50 % confidence level, and the *MR* can be approximated as:

$$MR = \left(\frac{i - 0.3}{N + 0.4} \right) \times 100 \qquad (1)$$

where i represents the order of failures in a group of test and N represents the total number of samples. E.g. for a test including 10 samples, by using MR the testing time when 2 samples fail will represent the lifetime with 16.3 % probability of failure, instead of 20 %.

From the MR, the uncertainty ξ under a sample size N can be calculated as:

$$\xi_{@N} = 1 - \left(MR_{max@N} - MR_{min@N} \right) \qquad (2)$$

where $MR_{max@N}$ and $MR_{min@N}$ are the highest and lowest median ranks with sample size of N. The uncertainty ξ with relation to the sample size N is plotted in Fig. 8.
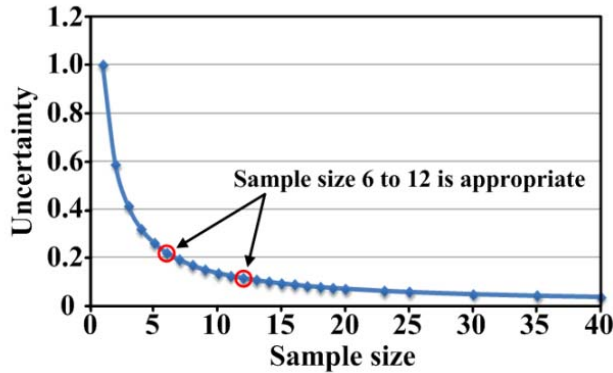

Fig. 8. The uncertainty ξ with relation to the sample size N.

The samples size can be decided depending on the required uncertainty level in the results. By examining Fig. 8, it is concluded that the sample size between 6 and 12 for a group of test is most cost-effective. In order to minimize the testing time, 6 samples are used in this paper to extract the strength information of device under each of the stress level shown in Table II, these conditions cover most of the interested stress behaviors under the given mission profile and application. As a result, 36 total samples of IGBT are needed for the strength tests – this sample size can ensure an uncertainty level at 20 %, and all of the testing conditions are closely related to the device loading in practical use.

6 DUTs are stressed under each of the testing condition in Table II until the devices satisfy the failure criteria, which defines that the static conduction voltage of transistor T_{VL} exceeds 5 % of the nominal value at loading current of 20 A. Afterwards the corresponding numbers of thermal cycles to the defined failures are recorded as the lifetime. In this test the cycling frequency or duration time of thermal cycles is considered as the stress level.

It is noted that the testing conditions shown in this paper are slightly accelerated in respect to the lifetime of IGBT, the testing conditions can be changed in order to further accelerate the testing time, in this case extrapolation of the tested results are needed, and larger prediction errors of reliability could be presented. However, by studying the interested stress profiles extracted from mission profiles, and by analyzing the required uncertainty at different testing samples, the testing effort can be significantly reduced.

B. Extracted CDF at one stress level

A testing example is shown in Fig. 9, in this test 6 IGBT modules are stressed under the testing condition 4 in Table II, and the conduction voltages of each DUT are recorded in Fig. 9 (a). The percentage of failure for a group of samples (by using MR) in relation to the number of thermal cycles (or operating time) is plotted in Fig. 9 (b). By fitting the testing points with a 2 parameters Weibull function with β=28.35 and η=203197 at 90 % confidence bound, the reliability function or CDF curve under the thermal cycle with 1 second duration time is

established. The MTTF of this group of samples is around 200 k thermal cycles, which are equivalent to 2.3 days of testing time.
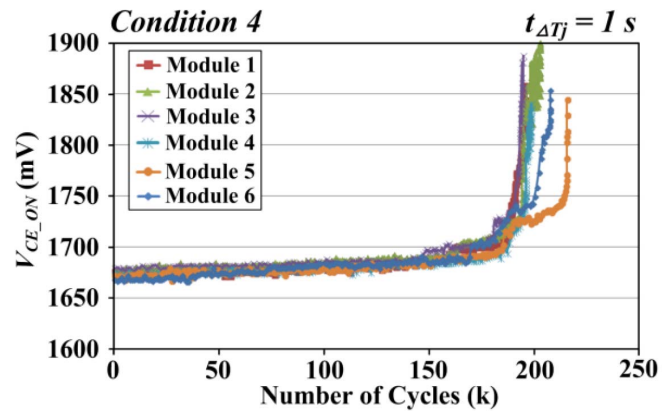
(a) Power cycling test results under one stress level
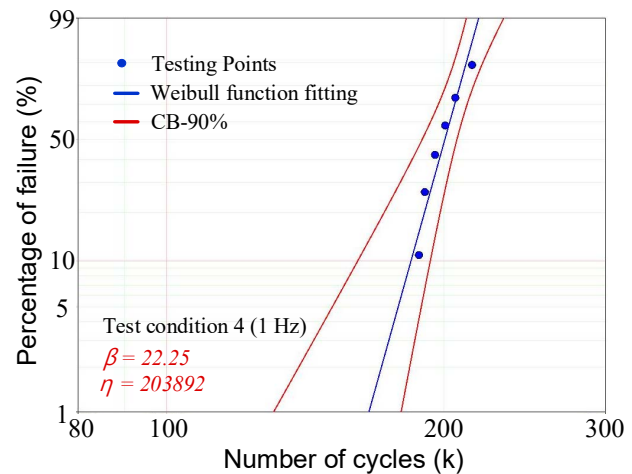
(b) CDF curve and Weibull fitting under one stress level

Fig. 9. A group of IGBT modules tested under a stress level with cycling frequency 1 Hz, testing condition 4 shown in Table II.

C. CDFs at multiple stress levels and model for CDF-stress levels relationship

By repeating the similar testing process on each of the testing conditions shown in Table II, the CDF curves of the IGBT module under different stress levels, in this case the duration times of thermal cycle, can be generated. The relationship between the Bx lifetime (number of thermal cycles to x % probability of failure: $NF_{@Bx}$) and stress level (duration time of thermal cycling: t_{period}) is fitted with a lifetime model (3) with fitting parameters of a, b and n [54]. As an example illustrated in Fig.10, the lifetime model at 10 % probability of failure is shown. The fitting parameters of the lifetime models under different probabilities of failure are summarized in Table. III, which is a strength model of power semiconductor device with more reliability information.

$$NF_{@Bx}(t_{period}) = \frac{a_{@Bx} + b_{@Bx} \cdot (t_{period})^{-n}}{a_{@Bx} + 1} \qquad (3)$$
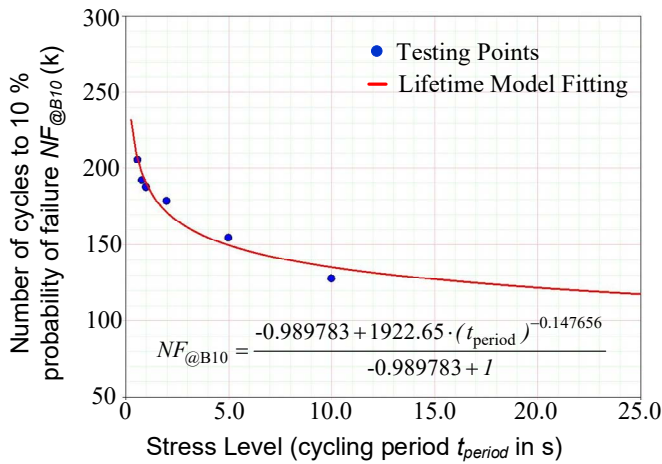
Fig. 10. B10 Lifetime model of IGBT modules tested under different stress levels of cycling period with testing conditions shown in Table II.

Table III. Fitting parameters for the lifetime model of DUT under different probabilities of failure.

Probability of failure (%)	Fitting parameters in (3)		
	a	b	n
1	-0.990124	1653.251685	0.159895
10	-0.989783	1922.651603	0.147656
20	-0.989940	1963.800773	0.143583
30	-0.990089	1979.247972	0.141000
40	-0.990210	1990.952300	0.139749
50	-0.990228	2017.864059	0.137350
60	-0.990233	2044.732327	0.135768
70	-0.990209	2077.623781	0.134199
80	-0.990153	2119.860095	0.132541

VI. MAPPING AND DEDUCTION OF RELIABILITY METRICS

A simplified mission profile of the testing setup based on a motor drive application is first defined as a study case, as shown in Fig. 11. The converter is stressed with variable load for 24 hours, which are repeated until the failure criteria of IGBT module is identified. This mission profile is composed of three sections of thermal cycles at different frequencies, i.e. 1 Hz running for 4 hours (t_{period} =1 s), 0.5 Hz running for 5 hours (t_{period} =2 s), and 0.15 Hz running for 15 hours (t_{period} =6.66 s). The amplitude and mean value of thermal cycles are kept constant in the three sections at 80 K and 100 º C respectively.
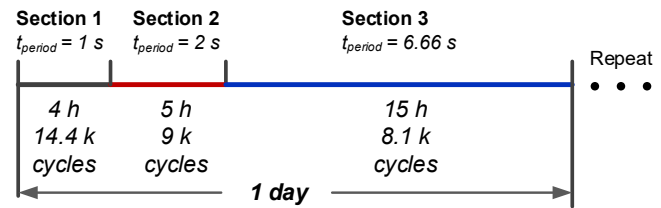

Fig. 11. A mission profile with combined thermal cycling frequencies for the testing setup.

A. Mapping of CDF based on stress profile and strength model

Because the stress intensities of t_{period} can be easily identified in the mission profile, it is possible to predict the time-to-failure information of component through (3). The quantified damage of the 1-day mission profile $D_{1day@Bx}$ (in the unit of %) which is composed of damages built in three sections, is calculated in (4) according to the "Miner's rule" [49] – this rule assumes that the damage built by each of the stress cycle can be accumulated, and the total accumulated damage is 1 when the component fails.

$$D_{1day@B_x} = D_{section1@B_x} + D_{section2@B_x} + D_{section3@B_x}$$
$$= \frac{14400}{NF_{@B_x}(t_{period\_section1})} + \frac{9000}{NF_{@B_x}(t_{period\_section2})} + \frac{8100}{NF_{@B_x}(t_{period\_section3})} \tag{4}$$

where $NF_{@Bx}$ represents the number of cycles to failure at certain probability of failure, $NF_{@Bx}$ can be found from Table III and equation (3).

If assuming the device is repeatedly loaded with the given mission profiles in Fig. 11, the lifetime of component at certain probability of failure $L_{@Bx}$ under the given mission profile can be calculated as:

$$L_{@B_x} = \frac{1}{D_{1day@B_x}}(day) \tag{5}$$

Taking into account (3)-(5) and Table III, the damage-developments in 1 day $D_{1day@Bx}$ and the predicted lifetimes $L_{@Bx}$ under the given mission profile, are plotted in Fig. 12, where the conditions with different probabilities of failure (from B1 to B80) are indicated.
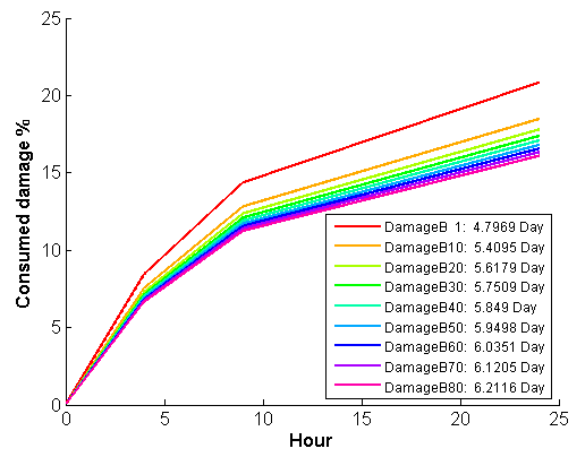

Fig. 12. Predicted accumulated damage of the DUT under different probabilities of failure based on the mission profiles in Fig. 11.

Consequently, the lifetimes of DUT are extracted under different probabilities of failures, and then the quantified CDF curve of DUT under the given mission profiles is predicted, as illustrated in Fig. 13, where the 2 parameters Weibull function with β=19.56 and η=6.062 is used to fit the CDF curve.
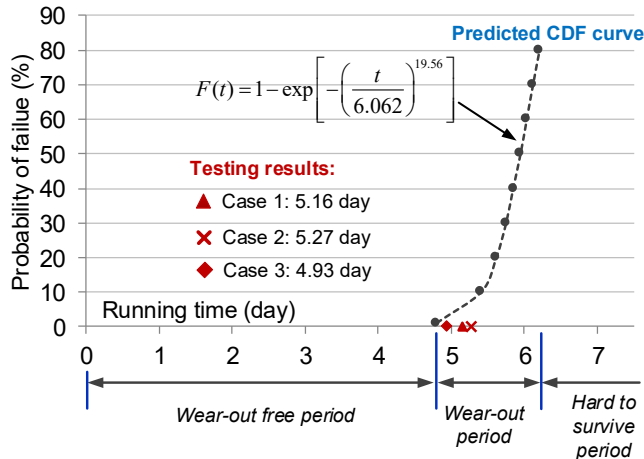

Fig. 13. Predicted CDF curve of the DUT based on the given mission profiles in Fig. 11 (3 testing results and Weibull function parameters are indicated).

B. Deduction of other reliability metrics based on CDF

The CDF curve shown in Fig. 13 contains full information of reliability performance, other important reliability metrics can be deducted from it. For example, the failure-rate $\lambda(t)$ (or hazard rate), which describes the frequency with which a system or component fails, can be deducted based on (6) and plotted in Fig. 14 (referred as quantified "bathtub curve") [50]. The Probability Density Function (PDF) curve, which is another important reliability metrics describing the probability distribution of the failure time, can be deduced based on (7) and plotted in Fig. 15 [39]:

$$\lambda(t) = \frac{1}{1-F(t)} \frac{dF(t)}{dt} \qquad (6)$$

Similarly, the metrics used in the conventional approaches for reliability assessment can be also deducted. The MTTF of DUT under the given mission profile can be deduced from the CDF function by (8), and it represents the average time that a group of samples fails. The Bx lifetime of DUT under the given mission profile can be easily found from Fig. 13. The predicted reliability metrics of the DUT under the given mission profiles of Fig. 11 are summarized in Table IV.

$$MTTF = \int_0^\infty \left[1 - F(t)\right] dt \qquad (8)$$

Compared to the CDF shown in Fig. 13, MTTF and Bx lifetime are over-simplified constants, which are independent of time and lose the whole picture of the reliability performance such as failure distribution and failure speed. As a result, benchmarking the systems or components by using MTTF or Bx lifetime is not recommended if the reliability function or CDF curve can be generated.

The quantified reliability metrics of Table IV and Fig.13-Fig. 15 is very useful information enabling new possibilities to evaluate the performances of power electronics converter. For
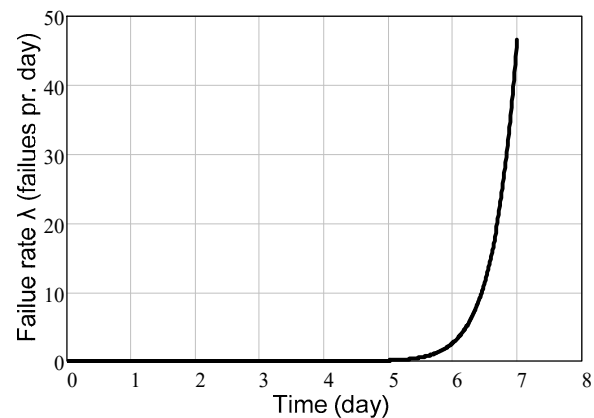
$$f(t) = \frac{dF(t)}{dt} \qquad (7)$$

Fig. 14. Predicted failure rate or "bathtub curve" for the DUT based on the given mission profile in Fig. 11.
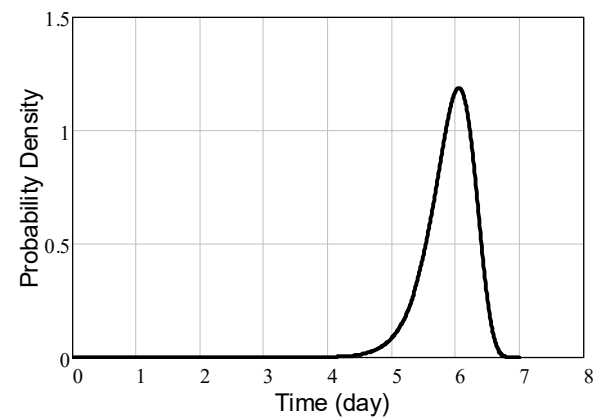

Fig. 15. Predicted Probability Density Function (PDF) for the DUT based on the given mission profile in Fig. 11.

example, in Table IV, by examine the value of β in the Weibull function and the failure rate curve in Fig. 14, the failure type under the testing conditions can be identified as the intensive wear-out failure starting from the 5th day. By looking at the CDF curve in Fig. 13, the accurate periods when the converter is in the status of wearing-out free, wearing-out, as well as hard-to-survive are clearly defined – this information can be used as the design targets or maintenance schedules of products, and these features are hard to be achieved by the existing reliability prediction approaches targeting for MTTF and Bx lifetime.

It is worth to mention that the reliability metrics extracted in this paper is a quantified benchmark for the reliability performance of converters under a specified failure mechanism (i.e. bond-wire wear-out failures of IGBT module triggered by various fundamental frequencies of thermal cycles). The reliability metrics for other components and wear-out failure mechanisms of power electronics can be generated by following the similar prediction process shown in Fig. 1. However, the used models to translate the mission profiles, as well as the testing methods to represent the strength of components, need to be explored in future work.

Table IV. Predicted reliability metrics for the DUT.

| Reliability metrics	Value
β in Weibull function	19.56
η in Weibull function	6.062
γ in Weibull function	0
Failure type	Wear out
MTTF	5.895 day
B10 lifetime	5.4 day

VII. Validation of the predicted reliability metrics

Long term reliability validation at months or years with acceptable efficiency is still a challenging task, which involves many other different activities such as monitoring techniques of converter health as well as long term warranty data from the manufacturers, these research topics are too large for this paper. As a result, the reliability validations are mostly done under different levels of accelerated and calibrated testing conditions in order to save the validation efforts, and then the reliability information under normal conditions can be extrapolated by different methods in the reliability engineering. Although there exits inevitable uncertainty in this extrapolation approach, it is generally believed that the reliability metrics under accelerated conditions can uncover many useful information of the converters, and can be used to benchmark different converter designs in respect to the reliability performances.

The mission profile shown in Fig. 11 is applied on the testing setup to validate the predicted reliability metrics. The static conduction voltage is online-monitored during the PWM operation of the converter. The detected conduction voltages of the transistors in the three phases of DUT are shown in Fig. 16 (a), which is corresponding to the defined mission profile, and the three loading sections are clearly identified. It can be seen that from the fifth day, there is a significant increase of the conduction voltage on T_{VL}, and at the testing time of 7430 minutes (5.16 days), the failure criteria is satisfied. A second test conducted is shown in Fig. 16 (b), in which the failure criteria is satisfied at 7600 minutes (5.27 days) of testing time.

Another test is conducted with similar loading conditions of Fig. 11, but different loading sequence as Section 3–1–2. According to the Miner's rule, this loading sequence will result in the same accumulated damage and reliability performances. The experimental results are shown in Fig. 16 (c), and it can be seen that at 7100 minutes (4.93 days) of testing time, the failure criteria is satisfied.
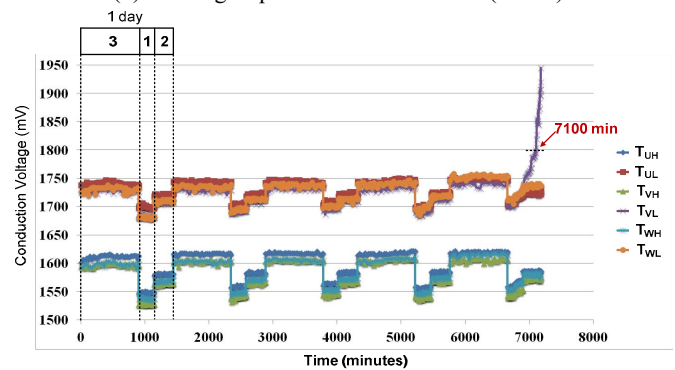
The recorded lifetimes from the tests is plotted in Fig. 13, and it is concluded that all of them are well located within the range of predicted period for wear-out failures, and the predicted reliability metrics show good accuracy.
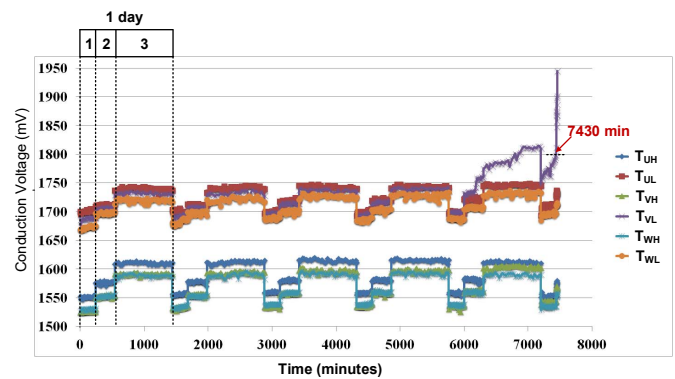
(a)　Loading sequence of Section1-2-3 (case 1).
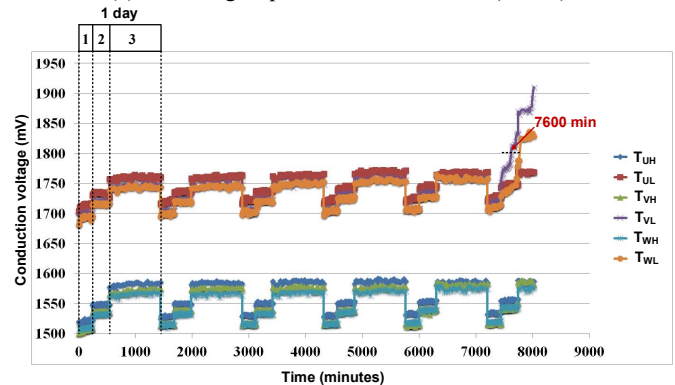
(b) Loading sequence of Section 1-2-3 (case 2).

(c) Loading sequence of Section 3-1-2 (case 3).

Fig. 16. Measured conduction voltage of the transistors in the three phase of DUT under continuous thermal cycling test.

VIII. Conclusions

The quantified reliability metrics based on the mission profiles and converter design is essential information to achieve cost-effective converter design. In this paper, a more advanced metric "Cumulative Distribution Function (CDF)" is introduced to predict the reliability performance of power electronics system based on mission profiles in motor drive application, and then a flow to extract the CDF is demonstrated. Furthermore, the accuracy of the predicted reliability metrics is verified through a series of wear-out tests in a converter testing system. It is concluded that the CDF is a very suitable metric to predict the reliability performance of converter, and it has shown good accuracy with much more reliability information compared to the existing approaches. In this method, the correct stress translation and dedicated strength tests based on mission

profiles are two key factors to ensure the efficiency and accuracy of reliability prediction.

REFERENCE

[1] F. Blaabjerg, K. Ma, "Future on power electronics for wind turbine systems," *IEEE Journal of Emerging and Selected Topics in Power Electronics*, vol. 1, no. 3, pp. 139-152, 2013.

[2] K. Ma, U. Choi, F. Blaabjerg, "Reliability Metrics Extraction for Power Electronics Converter Stressed by Thermal Cycles," in *Proc. of IEEE ECCE 2017*, pp. 3838-3843, Oct 2017.

[3] H. Wang, M. Liserre, F. Blaabjerg, P. Rimmen, J. Jacobsen, T. Kvisgaard, J. Landkildehus, "Transitioning to physics-of-failure as a reliability driver in power electronics", *IEEE Journal of Emerging and Selected Topics in Power Electronics*, vol. 2, no. 1, pp. 97-114, Mar 2014.

[4] K. Ma, D. Zhou, F. Blaabjerg, "Evaluation and Design Tools for the Reliability of Wind Power Converter System," *Journal of Power Electronics*, Vol. 15, No. 5, pp. 1149-1157, 2015.

[5] H. Wang, H. Chung, F. Blaabjerg, and M. Pecht, *Reliability engineering in power electronic converter systems*, Reliability of Power Electronic Converter Systems, IET, Dec. 2015.

[6] S. Faulstich, P. Lyding, B. Hahn, P. Tavner "Reliability of offshore turbines–identifying the risk by onshore experience," in *Proc. of European Offshore Wind*, Stockholm, 2009.

[7] L. M. Moore and H. N. Post, "Five years of operating experience at a large, utility-scale photovoltaic generating plant," Journal *of Prog. Photovolt: Res. Appl.* vol. 16, no. 3, pp. 249-259, 2008.

[8] Military Handbook: *Reliability prediction of electronic equipment*, MIL-HDBK-217F, Dec. 2, 1991.

[9] R. B. Abernethy, *The new Weibull handbook, fifth edition*, SAE International, 2007.

[10] G. F. Watson, "MIL Reliability: a new approach", *IEEE Spectrum*, Vol. 29, No. 8, pp. 46-49, 1992.

[11] S.V. Dhople, A. Davoudi, A.D. Dominguez-Garci and P. L. Chapman, "A unified approach to reliability assessment of multiphase DC-DC converters in photovoltaic energy conversion systems," *IEEE Trans. on Power Electronics*, vol. 27, no. 2, pp. 739- 751, Feb. 2012.

[12] R. Burgos C. Gang, F. Wang, D. Boroyevich, W. G. Odendaal and J. D. V. "Reliability-oriented design of three-phase power converters for aircraft applications," *IEEE Transactions on Aerospace Electronics System*, vol. 48, no. 2, pp. 1249-1263, Apr. 2012.

[13] M. G. Pecht, F. R. Nash, "Predicting the reliability of electronic equipment," *Proceedings of the IEEE*, Vol. 82, No. 7, pp. 992-1004, 1994.

[14] J. Colmenares, D. P. Sadik, P. Hilber, H. P. Nee, "Reliability Analysis of a High-Efficiency SiC Three-Phase Inverter", *IEEE Journal of Emerging and Selected Topics in Power Electronics*, Vol. 4, No. 3, pp. 996-1006, 2016.

[15] F. Chan, H. Calleja, "Reliability Estimation of Three Single-Phase Topologies in Grid-Connected PV Systems," *IEEE Transaction on Industrial Electronics*, Vol. 58, No. 7, pp. 2683-2689, 2011.

[16] D. Hirschmann, D.Tissen, S. Schröder, R. W. De Doncker, "Reliability Prediction for Inverters in Hybrid Electrical Vehicles", *IEEE Transaction on Power Electronics*, Vol. 22, No. 6, pp. 2511-2517, 2007.

[17] ZVEL, *Handbook for robustness validation of automotive electrical/electronic modules*, revised version, Jun. 2013.

[18] W. Denson, "The history of reliability prediction," *IEEE Transactions on Reliability*, Vol. 47, No. 3, pp. 321-328, 1998.

[19] A. Dasgupta, M. Pecht, "Material failure mechanisms and damage models", *IEEE Transactions on Reliability*, Vol. 40, No. 5, pp.531-536, 1991.

[20] E. Wolfgang, "Examples for failures in power electronics systems," presented at *ECPE Tutorial on Reliability of Power Electronic Systems*, Nuremberg, Germany, April 2007.

[21] S. Yang, A. T. Bryant, P. A. Mawby, D. Xiang, L. Ran, and P. Tavner, "An industry-based survey of reliability in power electronic converters," *IEEE Trans. on Ind. Appl.*, vol. 47, no. 3, pp. 1441- 1451, May/Jun. 2011.

[22] M. Ciappa, "Selected failure mechanisms of modern power modules," *Microelectronics Reliability*, vol. 42, no. 4-5, pp. 653-667, Apr.-May 2002.

[23] D. Simon, C. Boianceanu, G. D. Mey, V. Topa, A. Spitzer, "Reliability Analysis for Power Devices Which Undergo Fast Thermal Cycling," *IEEE Transactions on Device and Materials Reliability*, Vol. 16, No. 3, pp. 336-344, 2016.

[24] L. R. GopiReddy, L. M. Tolbert, B. Ozpineci, "Power Cycle Testing of Power Switches: A Literature Survey," *IEEE Transactions on Power Electronics*, Vol. 30, No. 5, pp. 2465-2473, 2015.

[25] C. Durand, M. Klingler, D. Coutellier, H. Naceur, "Power Cycling Reliability of Power Module: A Survey," *IEEE Transactions on Device and Materials Reliability*, Vol. 16, No. 1, pp. 80-97, 2016.

[26] W. B. Nelson, *Accelerated testing – statistical models, test plans, and data analysis*, Hoboken: John Wiley & Sons, 2004.

[27] General Motors Corporation Handbook GMW8758, *calibrated accelerated life testing*, 2004.

[28] M. Held, P. Jacob, G. Nicoletti, P. Scacco, M. H. Poech, "Fast power cycling test for IGBT modules in traction application," *in Proc. Power Electronics and Drive Systems*, pp.425-430, 1997.

[29] H. Berg and E. Wolfgang, "Advanced IGBT modules for railway traction applications: Reliability testing," *Microelectronics Reliability*, vol. 38, no. 6-8, pp. 1319-1323, Jun.-Aug., 1998.

[30] V. Smet, V., F. Forest, J.J. Huselstein, "Ageing and failure modes of IGBT modules in high-temperature power cycling," *IEEE Trans. Industrial Electronics*, vol. 58, no. 10, pp. 4931-4941, Oct. 2011.

[31] Aaron Hutzler, et al., "Power cycling community 1995-2014 - An overview of test results over the last 20 years," *Bodo's power systems*, May 2014.

[32] J. Berner, "Load-cycling capability of HiPak IGBT modules," ABB Application Note 5SYA 2043-02, 2012.

[33] U. Scheuermann, Ralf Schmidt, "A New Lifetime Model for Advanced Power Modules with Sintered Chips and Optimized Al Wire Bonds," *Proc. of PCIM' 2013*, pp. 810-813, 2013.

[34] T. E. Salem, R. A. Wood, "1000-H Evaluation of a 1200-V, 880-A All-SiC Dual Module," *IEEE Transactions on Power Electronics*, Vol. 29, No. 5, pp. 2192-2198, 2014.

[35] P. D. Reigosa, H. Wang, Y. Yang, and F. Blaabjerg, "Prediction of bond wire fatigue of IGBTs in a PV inverter under a long-term operation," *IEEE Trans. Power Electronics*, vol. 31, no. 10, pp. 7171-7182, Oct. 2016.

[36] K. Ma, M. Liserre, F. Blaabjerg, T. Kerekes, "Thermal Loading and Lifetime Estimation for Power Device Considering Mission Profiles in Wind Power Converter," *IEEE Trans. on Power Electronics*, Vol. 30, No. 2, pp. 590-602, 2015.

[37] L. Wei, J. McGuire, R. A. Lukaszewski, "Analysis of PWM Frequency Control to Improve the Lifetime of PWM Inverter", *IEEE Trans. on Industry Applications,* Vol. 47, No. 2, pp. 922-929, 2011.

[38] M. Musallam, C. Yin, C. Bailey, M. Johnson, "Mission Profile-Based Reliability Design and Real-Time Life Consumption Estimation in Power Electronics," *IEEE Trans. on Power Electronics*, Vol. 30, No. 5, pp. 2601-2613, 2015.

[39] P. O'Connor and A. Kleyner, *Practical reliability engineering*, the 5th edition, West Sussex: John Wiley & Sons, 2012.

[40] W. Weibull, "Statistical distribution function of wide applicability," *ASME Journal of Applied Mechanics*, vol. 18, no. 3, pp. 293-297, Sep. 1951.

[41] K. Ma, H. Wang, F. Blaabjerg, "New Approaches to Reliability Assessment: Using physics-of-failure for prediction and design in power electronics systems," *IEEE Power Electronics Magazine*, Vol. 3, No. 4, pp. 28-41, 2016.

[42] U. Choi, S. Jørgensen, and F. Blaabjerg, "Advanced accelerated power cycling test for reliability investigation of power device modules," *IEEE Trans. on Power Electronics*, vol. 31, no. 12, pp. 8371- 8386, Dec. 2016.

[43] B. Wu, M. Narimani, *High-Power Converters and AC Drives,* 2rd edition, IEEE Press & Wiley, ISBN: 978-1-119-15603-1, 2017.

[44] K. Ma, F. Blaabjerg, "Multi-timescale modelling for the loading behaviors of power electronics converter" *in Proc. of IEEE ECCE 2015*, pp. 5749-5756, 2015.

[45] A. Bahman, K. Ma, P. Ghimire, F. Iannuzzo, F. Blaabjerg, "A 3D Lumped Thermal Network Model for Long-term Load Profiles Analysis in High Power IGBT Modules" *IEEE Journal of Emerging and Selected Topics in Power Electronics, Vol. 4, No. 3, pp. 1050-1063,2016.*

[46] K. Ma, N. He, M. Liserre, F. Blaabjerg, "Frequency-Domain Thermal Modelling and Characterization of Power Semiconductor Devices," *IEEE Trans. on Power Electronics*, Vol. 31, No. 10, pp. 7183-7193, 2016.

[47] A. Wintrich, U. Nicolai, T. Reimann, "Semikron Application Manual," 2015.

[48] U. Choi, F. Blaabjerg, and S. Jørgensen, "Study on Effect of Junction Temperature Swing Duration on Lifetime of Transfer Molded Power IGBT Modules," *IEEE Trans. on Power Electronics*, Vol. 32, No. 8, pp. 6434-6443, 2017.

[49] M. A. Miner, "Cumulative damage in fatigue," *Journal of Applied Mechanics*, no. 12, A159-A164, 1945.

[50] G.A. Klutke, P.C. Kiessler, M.A. Wortman, "A critical look at the Bathtub curve," *IEEE Transaction on Reliability*, Vol. 52, No. 1, pp. 125-129, 2003.

[51] W. Lai, M. Chen, L. Ran, S. Xu, N. Jiang, X. Wang, O. Alatise, P. Mawby, "Experimental Investigations on the Effects of Narrow Junction Temperature Cycles on Die-attach Solder Layer in an IGBT Module," *IEEE Trans. on Power Electronics*, vol. 32, no. 2, pp. 1431-1441, 2017.

[52] L. Yang, P. A. Agyakwa, C. M. Johnson, "Physics-of-Failure Lifetime Prediction Models for Wire Bond Interconnects in Power Electronic Modules," *IEEE Transactions on Device and Materials Reliability*, vol. 13, no. 1, pp. 9-17, 2013.

[53] M. A. Eleffendi, C. M. Johnson, "In-Service Diagnostics for Wire-Bond Lift-off and Solder Fatigue of Power Semiconductor Packages," *IEEE Trans. on Power Electronics*, vol. 32, no. 9, pp. 7187-7198, 2017.

[54] L. A. Escobar, W. Q. Meeker, "A review of accelerated test models," *Statist. Sci.*, vol. 21, no. 4, pp. 552–577, 2006.